T–Ω Formulation for Eddy-Current Problems with Periodic Boundary Conditions

Paolo Bettini[1,2], Roberto Benato[1], Sebastian Dambone Sessa[1], and Ruben Specogna[3]

[1]Department of Industrial Engineering, University of Padova, 35131 Padua, Italy
[2]Consorzio RFX, 35127 Padua, Italy
[3]Polytechnic Department of Engineering and Architecture, Università di Udine, 33100 Udine, Italy

This paper presents a novel technique to perform the topological pre-processing needed in formulations based on an electric vector potential and a magnetic scalar potential when the eddy-current problem being solved is subject to periodic boundary conditions. In this case, in fact, all the techniques to produce the generators for the first cohomology group introduced in the literature cannot be used directly on the input mesh. The novel technique is very fast and it is used to model cables for power delivery.

***Index Terms*— Cohomology, cuts, eddy currents, magnetic scalar potential, periodic boundary conditions (PBCs).**

I. Introduction

ONE of the most attractive ways to solve eddy-current problems is the T–Ω finite-element formulation. Its efficiency originates from the fact that the magnetic field is irrotational in the insulating region and a magnetic scalar potential can, therefore, be used. Yet, when the insulating region is topologically non-trivial (for example, is the complement of a conductor which is a torus), then topology starts to play a role, and, by definition, what is needed is a set of so-called generators that form a basis of the first cohomology group of the insulating region [1], [2].

This issue remained an open problem for many years. Recently, faster computers, novel algorithms, and implementations are able to provide these generators in a time that is negligible with respect to the other parts of the simulation chain (for example, meshing or solving the linear system). In particular, one of the fastest techniques to perform the topological pre-processing required for T–Ω formulation is the Dłotko–Specogna (DS) algorithm introduced in [3] and [4].

This contribution extends the DS algorithm in order to deal with problems with periodic boundary conditions (PBCs), which can arise in many applications of interest.

This paper is organized as follows. In Section II, we recall the T–Ω formulation and introduce the novel approach to deal with PBCs. In Section III, we describe how the PBC is implemented. In Section IV, we present the numerical results on some benchmark problems. Finally, in Section V, the conclusions are drawn.

II. T–Ω Geometric Formulation

The domain of interest D of the eddy-current problem has been partitioned into a source region D_s, in a passive conductive region D_c and the air region D_a. In this section, we assume D_c to be simply connected.

We cover the domain D with a polyhedral mesh forming the primal complex $\mathcal{K}$ whose oriented geometric elements are nodes n, edges e, faces f, and volumes v. $\mathcal{K}_s$, $\mathcal{K}_c$, and $\mathcal{K}_a$ represent the sub-complexes of $\mathcal{K}$ relative to geometric elements belonging to D_s, D_c, and D_a, respectively. The interconnections of complex $\mathcal{K}$ are described with incidence matrix $\mathbf{G}$ between edges and nodes, $\mathbf{C}$ between faces and edges, and $\mathbf{D}$ between elements and faces. In this paper, subscripts c, s, and a denote the restriction of an array or a matrix to the geometric elements in $\mathcal{K}_c$, $\mathcal{K}_s$, and $\mathcal{K}_a$, respectively.

By means of the barycentric subdivision of $\mathcal{K}$, a dual complex $\tilde{\mathcal{K}}$ is constructed [5], whose geometric elements are dual volumes $\tilde{v}$, dual faces $\tilde{f}$, dual edges $\tilde{e}$, and dual nodes $\tilde{n}$ in a one-to-one correspondence (duality) with the geometric elements of $\mathcal{K}$, respectively. The matrices $\tilde{\mathbf{G}} = \mathbf{D}^T$, $\tilde{\mathbf{C}} = \mathbf{C}^T$, and $\tilde{\mathbf{D}} = -\mathbf{G}^T$ describe the mutual interconnections between the geometric elements of $\tilde{\mathcal{K}}$.

Let us now consider the integrals of the fields involved in the eddy-current problem with respect to the oriented geometric elements of $\mathcal{K}$ and $\tilde{\mathcal{K}}$. We introduce the following arrays of degrees of freedom (DoFs).

1) $\boldsymbol{\Phi}$ denotes the array of magnetic induction fluxes, where each flux is associated with a face $\tilde{f} \in \mathcal{K}$.
2) $\mathbf{F}$ is the array of magneto-motive forces associated with $e \in \mathcal{K}$.
3) $\mathbf{I}$ is the array of electric currents associated with $f \in \mathcal{K}_c$.
4) $\mathbf{U}$ is the array of electro-motive forces along edges $\tilde{e} \in \mathcal{K}$.
5) Finally, the array $\mathbf{I}^e$ of known source (excitation) currents is considered with $f \in \mathcal{K}$ (different from zero only in the source region $\mathcal{K}_s$).

With symbol $(\bullet)_x$, with $x \in \{f, e, n, \tilde{f}, \tilde{e}\}$, we denote the component of an array indexed by x.

According to the discrete geometric approach, Maxwell's laws can be enforced exactly on a given mesh as balance equations involving the DoFs arrays of the complex $\tilde{\mathcal{K}}$ or $\mathcal{K}$.

Manuscript received November 20, 2016; revised December 28, 2016; accepted January 12, 2017. Date of publication January 17, 2017; date of current version May 26, 2017. Corresponding author: P. Bettini (e-mail: paolo.bettini@unipd.it).

Color versions of one or more of the figures in this paper are available online at http://ieeexplore.ieee.org.

Digital Object Identifier 10.1109/TMAG.2017.2654498

0018-9464 © 2017 IEEE. Personal use is permitted, but republication/redistribution requires IEEE permission.
See http://www.ieee.org/publications_standards/publications/rights/index.html for more information.

Therefore, in the frequency domain, Gauss' magnetic law and Faraday's law can be enforced on the dual complex with

$$\begin{aligned} \mathbf{G}^T\boldsymbol{\Phi} &= \mathbf{0} \quad \text{(a)}\\ \mathbf{C}^T\mathbf{U} &= -i\omega\boldsymbol{\Phi} \quad \text{(b).} \end{aligned} \tag{1}$$

In order to satisfy continuity law implicitly in $\mathcal{K}_c$ and $\mathcal{K}$

$$\begin{aligned} \mathbf{D}_c\mathbf{I} &= \mathbf{0} \text{ (a)}\\ \mathbf{D}\mathbf{I}^e &= \mathbf{0} \text{ (b)} \end{aligned} \tag{2}$$

we introduce the arrays $\mathbf{T}$ and $\mathbf{T}^e$ of the circulations of the electric vector potential T along the edges $e \in \mathcal{K}_c$ and $e \in \mathcal{K}$, respectively, such that

$$\begin{aligned} \mathbf{C}_c\mathbf{T} &= \mathbf{I} \quad \text{(a)}\\ \mathbf{C}\mathbf{T}^e &= \mathbf{I}^e \quad \text{(b)} \end{aligned} \tag{3}$$

hold. In fact, we recall that $\mathbf{DC} = \mathbf{0}$ and $\mathbf{D}_c\mathbf{C}_c = \mathbf{0}$ hold. The array $\mathbf{T}^e$ can be computed by the extended spanning tree technique (ESTT) [6]. The ESTT is a general version of the Webb–Forghani iterative algorithm to find a discrete vector field whose discrete curl is assigned [7].

Ampère's balance law at discrete level yields to

$$\begin{aligned} \mathbf{C}_c\mathbf{F}_c &= \mathbf{I} \quad \text{(a)}\\ \mathbf{C}_s\mathbf{F}_s &= \mathbf{I}_s^e \quad \text{(b)}\\ \mathbf{C}_a\mathbf{F}_a &= \mathbf{0} \quad \text{(c).} \end{aligned} \tag{4}$$

From the definition of $\mathbf{T}$, $\mathbf{T}^e$, and the fact that $\mathbf{C}_x\mathbf{G}_x = \mathbf{0}$ holds for $x \in \{c, s, a\}$, (4) is equivalent to

$$\begin{aligned} \mathbf{F}_c &= \mathbf{G}_c\boldsymbol{\Omega}_c + \mathbf{T} + \mathbf{T}_c^e\\ \mathbf{F}_s &= \mathbf{G}_s\boldsymbol{\Omega}_s + \mathbf{T}_s^e\\ \mathbf{F}_a &= \mathbf{G}_a\boldsymbol{\Omega}_a + \mathbf{T}_a^e \end{aligned} \tag{5}$$

where we introduced an array $\boldsymbol{\Omega}$ of magnetic scalar potentials sampled in the nodes $n \in \mathcal{K}$.

The discrete counterparts of the constitutive material laws must be considered in addition to the discrete Maxwell's laws

$$\begin{aligned} \boldsymbol{\Phi} &= \mathbf{M}_\mu\,\mathbf{F} \text{ in } \mathcal{K} \quad \text{(a)}\\ \mathbf{U}_c &= \mathbf{M}_\rho\,\mathbf{I} \text{ in } \mathcal{K}_c \quad \text{(b)} \end{aligned} \tag{6}$$

where the square matrices $\mathbf{M}_\mu$ and $\mathbf{M}_\rho$ are efficiently constructed in a geometric and closed form as described in [5].

By substituting (6a), (6b), and (5) in (1a), the algebraic equations corresponding to the nodes in $\mathcal{K}$ are obtained. By substituting (6a), (6b), and (5) in (1b), the algebraic equations corresponding to edges in $\mathcal{K}_c$ are derived. The final algebraic system, having $\mathbf{T}$ and $\boldsymbol{\Omega}$ as unknown DoFs arrays, can be written as

$$\begin{aligned} (\mathbf{G}^T\mathbf{M}_\mu\mathbf{G}\boldsymbol{\Omega})_n + \left(\mathbf{G}_c^T\mathbf{M}_{\mu c}\mathbf{T}\right)_n + (\mathbf{G}^T\mathbf{M}_\mu\mathbf{T}^e)_n &= 0\\ \frac{1}{i\omega}\left(\mathbf{C}_c^T\mathbf{M}_\rho\mathbf{C}_c(\mathbf{T}+\mathbf{T}_c^e)\right)_e + \left(\mathbf{M}_{\mu c}\left(\mathbf{T}+\mathbf{T}_c^e+\mathbf{G}_c\boldsymbol{\Omega}_c\right)\right)_e &= 0 \end{aligned} \tag{7}$$

where the former is written $\forall n \in \mathcal{K}$ and the latter $\forall e \in \mathcal{K}_c$.

Finally, the interface conditions that avoid the current to flow outside region $\mathcal{K}_c$ are considered by setting the DoF of $\mathbf{T}$ to zero for all edges in $\partial\mathcal{K}_c$. In this way, $(\mathbf{I})_f = 0, \forall f \in \partial\mathcal{K}_c$ holds.

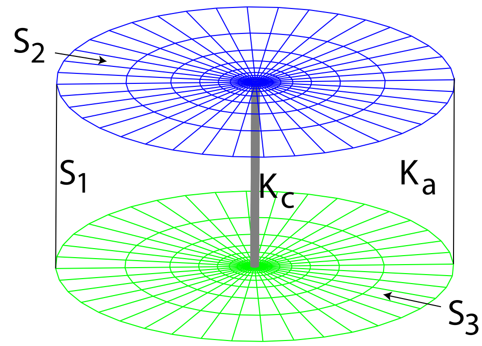

Fig. 1. Hexahedral mesh $\mathcal{K}$ constructed by sweeping a 2-D fine quadrilateral mesh. The passive conductive region is $\mathcal{K}_c$ and the nonconductive region $\mathcal{K}_a$. The mesh $\mathcal{K}$ is delimited by a cylindrical surface S_1 and two cap surfaces S_2 and S_3.

A. Non-Simply Connected Conductors and Periodic Boundary Conditions

In the proposed application, a hexahedral mesh $\mathcal{K}$ is constructed by sweeping a 2-D fine quadrilateral mesh on a path orthogonal to the 2-D mesh plane (see Fig. 1). The boundary of $\mathcal{K}$ is formed by the cylindrical surface S_1 and two cap surfaces S_2 and S_3 (see Fig. 1).

On S_2 and S_3 surfaces, we enforce the PBC. It means that we have to enforce all scalar and vector fields on S_2 and S_3 to be identical, due to the symmetry of the conductive structures. The two DoFs we consider are the magnetic scalar potential sampled on mesh nodes and the circulation of the electric vector potential on mesh edges in the interior of $\mathcal{K}_c$. The PBC is imposed by enforcing the value of these DoFs to be the same on the corresponding geometric elements of S_2 and S_3.

Now, we focus on the definition of potentials in $\mathcal{K}_a$ only. When the non-conducting region $\mathcal{K}_a$ is topologically non-trivial, the DoFs $\boldsymbol{\Omega}_a$ representing the magnetic scalar potential in the nodes of $\mathcal{K}_a$ are not enough to represent all possible magneto-motive forces $\mathbf{F}_a$ on mesh edges of $\mathcal{K}_a$. This is due to the fact that the magnetic field in $\mathcal{K}_a$ is curl-free but it cannot be represented by the gradient of a scalar potential given that its circulation on some loops in $\mathcal{K}_a$ made of mesh edges does not vanish. This is indeed the case if the loop links a conducting torus, since Ampère's law enforces that circulation to match the current that flows inside the conductive torus. It is possible to show [2] that the following definition of potentials in $\mathcal{K}_a$ holds in the general case:

$$\mathbf{F}_a = \mathbf{G}_a\boldsymbol{\Omega}_a + \mathbf{H}_a\mathbf{i} \tag{8}$$

where $\mathbf{G}_a$ as usual stores the incidences between edge and node pairs of $\mathcal{K}_a$ (i.e., the discrete gradient), $\mathbf{H}_a$ is a matrix that stores in its columns the representatives of the cohomology generators $H^1(\mathcal{K}_a)$ [2], [8], and $\mathbf{i}$ is an array that contains the *independent currents* [2]. The independent currents are, therefore, additional unknowns (DoFs) of the problem due to the topology of the conducting regions.

We recalled this definition of potentials to point out a constraint on the representatives of the cohomology generators due to the PBC that is not fulfilled, in general, by the techniques for performing the topological pre-processing proposed

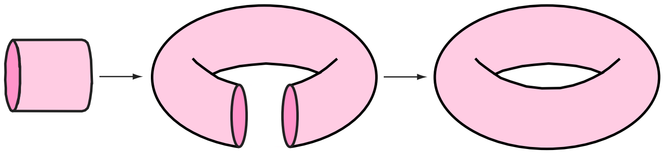

Fig. 2. Cylinder becomes a solid torus by topologically stitching the two caps of the cylinder.

in the literature. In fact, the representatives of generators must have the same trace on the two surfaces on which PBC is enforced.

This paper fills this gap by introducing an extension to the DS algorithm to guarantee that the aforementioned constraint is fulfilled. The main idea is to stitch topologically the two surfaces S_2 and S_3.

III. DS Algorithm and PBCs

In this section, we first describe how the PBC is implemented. Then, we present the idea and the pseudo-code of the modified DS algorithm.

A. PBCs Implementation

The PBC is enforced, in practice, during the usual elementwise assembly of the system matrix: the contributions from edges/nodes on S_2 are assembled unaltered, whereas the ones from edges on S_3 are assembled in the positions relative to the corresponding edges on S_2.

We note that this approach requires that each pair of coupled edges on S_2 and S_3 must have the same orientation. This constraint on edge orientation implies a constraint also on the nodes labels given that the canonical orientation of edges is based exactly on nodes labels. That is, we assume that the orientation of the edge e is such that $\mathbf{G}(e, n_1) = -1$ and $\mathbf{G}(e, n_2) = 1$, where $\mathbf{G}$ is the edge-node incidence matrix and n_1, n_2, with $n_1 < n_2$, are the integer labels of the two nodes in the boundary of e. Of course, mesh generators assign node labels that not necessarily meet this constraint.

We solve this issue by redistributing the labels on all mesh nodes as follows.

1) We define new labels on nodes on S_2 starting from 1 to N_2, where N_2 is the number of nodes on S_2.
2) Nodes labels on S_3 are then defined from N_2+1 to $2\,N_2$ by using the order of the corresponding nodes on S_2.
3) Finally, the labels of the nodes not belonging to $S_2 \cup S_3$ are redefined randomly, i.e., without a particular order.

B. Modified DS Algorithm

The main idea is to construct a new cell complex $\underline{\mathcal{K}}$ to compute cohomology with the DS algorithm by topologically stitching the mesh by gluing S_2 with S_3. For example, if we have a cylinder, with the proposed technique, we get a torus as graphically shown in Fig. 2. Of course, this stitching involves only the topology of the mesh; therefore, no deformation of the mesh occurs.

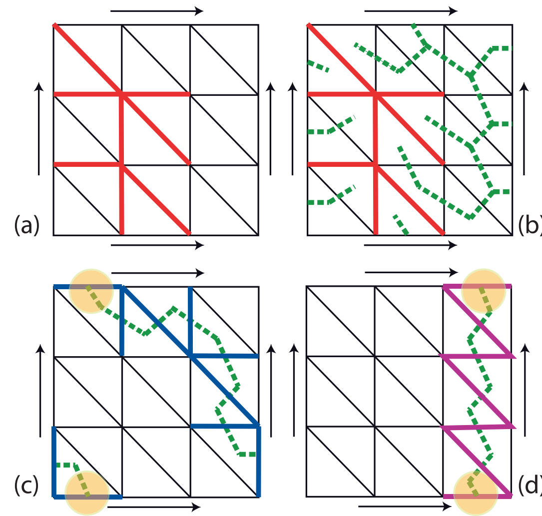

Fig. 3. (a) Edge spanning tree on $\mathcal{S}$. (b) Dual edge spanning tree on $\mathcal{S}$ is constructed by using as graph the dual edges whose dual are edges not in the primal tree. (c) and (d) Support of the two cohomology generators $H^1(\mathcal{S})$ produced by the two free edges indicated with circles in the picture.

Then, the DS algorithm [3], [4] is applied to the modified complex to obtain a set of lazy generators for the $H^1(\underline{\mathcal{K}}_a)$ basis, according to the following steps.

1) Find the $H^1(\mathcal{S})$ generators, where $\mathcal{S} = \underline{\mathcal{K}}_c \cap \underline{\mathcal{K}}_a$, as shown in Fig. 3.
2) Obtain the thinned currents by pre-multiplying by the face-edge incidence matrix $\underline{\mathbf{C}}_c$, where $\underline{\mathbf{C}}$ is the incidence matrix between faces and edges of $\underline{\mathcal{K}}$.
3) Run the ESTT in $\underline{\mathcal{K}}$ by considering the thinned current as current distribution.
4) Set to zero the coefficients that are eventually non-zero inside $\underline{\mathcal{K}}_c$.

IV. Numerical Results

This section shows the results on some benchmark problems to investigate the performances of the method proposed in this paper. We first consider a simple case consisting in a single straight conductor, because an analytical reference solution is available. Then, we present the results on a more complicated geometry, which mimics the typical strandings of the cores of a three-core armored cable.

Linear systems are all solved with Intel MKL PARDISO, given that it performs very well on multi-core systems.

A. Single Straight Conductor

We first consider a cylinder of 19.25 mm of radius, with a resistivity of $2.048 \cdot 10^{-8}$ Ωm and a current of 800 A (rms).

In Fig. 4, the representative of the cohomology $H^1(\mathcal{K}_a)$ generator is shown.

The convergence of the Joule power losses P inside the cable with mesh refinement is shown in Fig. 5. The accuracy of the T–Ω formulation with respect to the analytical reference is quite good. We include also the results of the A formulation based on the magnetic vector potential with current enforced by cohomology generators [9].

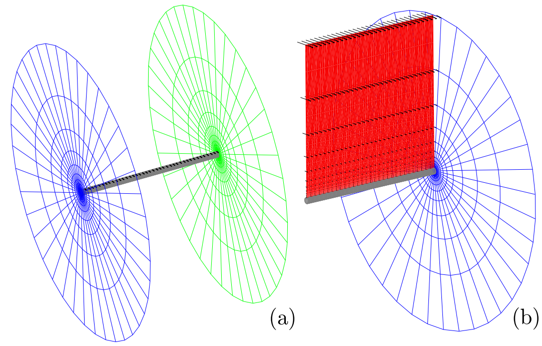

Fig. 4. (a) Geometry of the single straight conductor. (b) Support of the representative of the cohomology $H^1(\mathcal{K}_a)$ generator. The dual of its support is also shown in red.

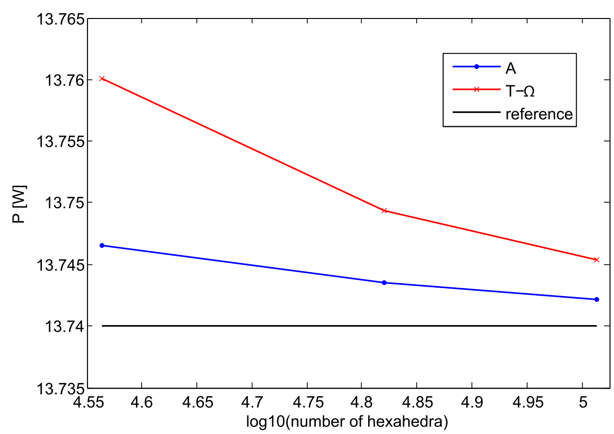

Fig. 5. Convergence versus mesh refinement of the dissipated power in the single conductor benchmark.

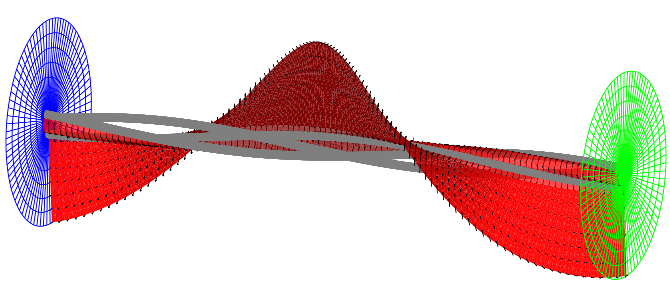

Fig. 6. Support of the representative of one of the cohomology generators $H^1(\mathcal{K}_a)$.

TABLE I
POWER LOSSES IN 3 m OF TWISTED CABLE

Formulaton	ndofs	total time [s]	Power losses [W]
T-Ω	643 000	320	133.82
A-V	916 903	1 020	133.56

B. Three Twisted Conductors

A more complicated benchmark of three twisted cables 3 m long is proposed. The mesh consists of 315 827 nodes, 939 910 edges, and 308 400 hexahedral elements. The support of one of the cohomology generators obtained in shown in Fig. 6.

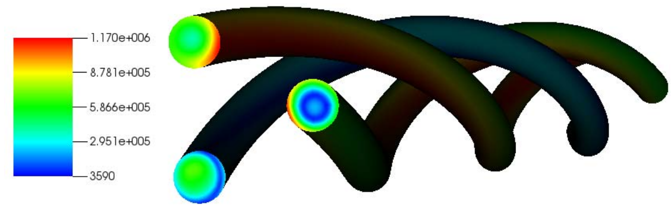

Fig. 7. Real component of the current density computed with the T–Ω formulation for the three twisted conductors.

The Joule power losses for the 3-m cable are shown in Table I, together with some data about the total number of DoFs and the total simulation wall time (total time) for both the T–Ω and A formulation. Fig. 7 shows the current density computed with the T–Ω formulation.

V. CONCLUSION

The computation of the cohomology generators requires in all cases just a couple of seconds, showing the effectiveness of the proposed method.

Having the results of both complementary formulations allows to know where the mesh should be refined and to gain confidence about the obtained results for example with the technique proposed in [10].

ACKNOWLEDGMENT

This work was supported by the University of Padova under Grant CPDA144817.

REFERENCES

[1] Z. Ren, "T-Ω formulation for eddy-current problems in multiply connected regions," *IEEE Trans. Magn.*, vol. 38, no. 2, pp. 557–560, Mar. 2002.
[2] P. Dłotko and R. Specogna, "Cohomology in 3D magneto-quasistatics modeling," *Commun. Comput. Phys.*, vol. 14, no. 1, pp. 48–76, Jul. 2013.
[3] P. Dłotko and R. Specogna, "Physics inspired algorithms for (co)homology computations of three-dimensional combinatorial manifolds with boundary," *Comput. Phys. Commun.*, vol. 184, no. 10, pp. 2257–2266, Oct. 2013.
[4] P. Dłotko and R. Specogna, "Lazy cohomology generators: A breakthrough in (co)homology computations for CEM," *IEEE Trans. Magn.*, vol. 50, no. 2, pp. 577–580, Feb. 2014.
[5] L. Codecasa, R. Specogna, and F. Trevisan, "A new set basis functions for discrete geometric approach," *J. Comput. Phys.*, vol. 229, no. 19, pp. 7401–7410, Sep. 2010.
[6] P. Dłotko and R. Specogna, "Efficient generalized source field computation for h-oriented magnetostatic formulations," *Eur. Phys. J. Appl. Phys.*, vol. 53, Feb. 2011, Art. no. 20801.
[7] J. P. Webb and B. Forghani, "A single scalar potential method for 3D magnetostatics using edge elements," *IEEE Trans. Magn.*, vol. 25, no. 5, pp. 4126–4128, Sep. 1989.
[8] J. R. Munkres, *Elements of Algebraic Topology*. Cambridge, MA, USA: Perseus Books, 1984.
[9] P. Dłotko, R. Specogna, and F. Trevisan, "Voltage and current sources for massive conductors suitable with the A-χ geometric formulation," *IEEE Trans. Magn.*, vol. 46, no. 8, pp. 3069–3072, Aug. 2010.
[10] E. Creusé, S. Nicaise, R. Tittarelli, "A guaranteed equilibrated error estimator for the A-ϕ and T-Ω magnetodynamic harmonic formulations of the Maxwell system," *IMA J. Numer. Anal.*, to be published, doi: https://doi.org/10.1093/imanum/drw026